Aerial Co-Manipulation With Cables: The Role of Internal Force for Equilibria, Stability, and Passivity

Marco Tognon, Chiara Gabellieri, Lucia Pallottino, and Antonio Franchi

***Abstract*—This letter considers the cooperative manipulation of a cable-suspended load with two generic aerial robots without the need of explicit communication. The role of the internal force for the asymptotic stability of the beam position-and-attitude equilibria is analyzed in depth. Using a nonlinear Lyapunov-based approach, we prove that if a nonzero internal force is chosen, then the asymptotic stabilization of any desired beam attitude can be achieved with a decentralized and communicationless master–slave admittance controller. If, conversely, a zero internal force is chosen, as done in the majority of the state-of-the-art algorithms, the attitude of the beam is not controllable without communication. Furthermore, we formally proof the output-strictly passivity of the system with respect to an energy-like storage function and a certain input–output pair. This proves the stability and the robustness of the method during motion and in nonideal conditions. The theoretical findings are validated through extensive simulations.**

***Index Terms*—Aerial systems: mechanics and control, mobile manipulation, multi-robot systems, distributed robot systems.**

I. Introduction

OVER the last decade unmanned aerial vehicles have risen the interest of a larger and larger audience for their wide application domain. Recently, aerial physical interaction, using aerial manipulators [1], [2] or exploiting physical links as cables [3], has become a very popular topic. One interesting and applicative problem is the aerial manipulation of large objects, for which cooperative approaches are usually applied because they allow to overcome the limited payload of a single platform, thus lifting larger and heavier loads [4].

Many works targeted this problem proposing different methods and solutions. In [5], [6] cooperative aerial transportation of a rigid and an elastic object is considered, respectively. In [7] the use of multiple flying arms is exploited to address the problem. Aerial manipulation via cables is another interesting solution since it can reduce the couplings between the load and the robot attitude dynamics. Examples of cooperative aerial manipulation using cables are studied in [8]–[10]. All these examples rely on a centralized control. Instead, a decentralized algorithm, as in [11], is more robust and scalable with respect to (w.r.t.) the number of robots.

However, the major bottleneck in decentralized algorithms is the explicit communication. Communication delays and packet losses can affect the performance and even the stability of the systems. Limiting the need for explicit communication allows to reduce the complexity as well. In [12] the authors proposed one of the first decentralized leader-follower algorithm without explicit communication, for objects transportation performed by mobile ground robots. Aerial cooperative transportation by two robots without explicit communication has been addressed also in [13] for a cable-suspended beam-like load, and a leader-follower paradigm has been proposed. Here the leader follows an external position reference, while the horizontal position of the follower is controlled with an admittance filter, trying to keep the cable always vertical (zero internal force). A similar approach has been proposed in [14] but relying on a visual feedback. However, those methods do not deal with the load pose control and do not provide a formal stability proof.

For the same system composed by two aerial robots carrying a cable suspended beam-like load (see Fig. 1 for a schematic representation), we propose a decentralized algorithm relying only on implicit communication. Our algorithm uses a master-slave architecture with an admittance filter on both robots (not only on the slave as in the related state of the art), to make the overall system compliant/robust to external disturbances.

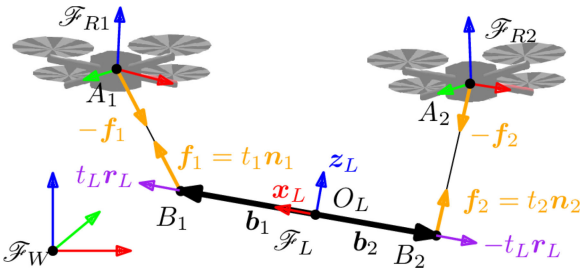

Fig. 1. Representation of the system and its major variables. The two aerial vehicles do not need to be necessarily quadrotors, since the analysis and control design is valid for general aerial vehicles.

Manuscript received September 10, 2017; accepted January 25, 2018. Date of publication February 8, 2018; date of current version April 11, 2018. This letter was recommended for publication by Associate Editor F. Ruggiero and Editor J. Roberts upon evaluation of the reviewers' comments. This work was supported by the European Union's Horizon 2020 research and innovation program under Grant 644271 AEROARMS. The first two authors have equally collaborated to this letter and can both be considered as first author. This paper is part of IEEE Robotics and Automation Letters' Special Issue on Aerial Manipulation, edited by F. Ruggiero, V. Lippiello, and A. Ollero. *(Corresponding author: Marco Tognon.)*

M. Tognon and A. Franchi are with the LAAS-CNRS, Université de Toulouse, 31400 Toulouse, France (e-mail: mtognon@laas.fr; antonio.franchi@laas.fr).

C. Gabellieri and L. Pallottino are with the Centro di Ricerca E. Piaggio, Università di Pisa, 56122 Pisa, Italy (e-mail: chiara.gabellieri@ing.unipi.it; lucia.pallottino@unipi.it).

This letter has supplementary downloadable material available at http://ieeexplore.ieee.org, provided by the authors. The Supplementary Materials contain a pdf file containing a technical report with additional simulation results, and a single movie file in MPEG-4 format. This material is 6.07 MB in size.

Digital Object Identifier 10.1109/LRA.2018.2803811

One of our main contributions is the constructive and intuitive method to choose the controller input to stabilize the load at a desired pose. The control of both position and orientation turns the simpler transportation task found in the state of the art in a full-manipulation one.

We show that those inputs are parametrized by the internal force of the load that plays a crucial role in the equilibria stability. Differently from the state of the art algorithms, which are not formally guaranteed to converge, we also provide a formal proof of the stability through Lyapunov's direct method. Furthermore, we prove that the controlled system is output-strictly passive w.r.t. a relevant input-output pair. This provides a bound for the energy variations during the manipulation and an index of robustness of the method.

In Section II we derive the model. In Section III we present the control strategy and the equilibria of the system. Their stability is discussed in Section IV. In Section V we prove the passivity and stability of transportation. Simulation results and conclusive discussions are presented in Sections VI and VII, respectively.

II. System Modeling

The considered system and its major variables are shown in Fig. 1. The beam-like *load* is modeled as a rigid body with mass $m_L \in \mathbb{R}_{>0}$ and a positive definite inertia matrix $\boldsymbol{J}_L \in \mathbb{R}^{3\times3}$. We define the frame $\mathcal{F}_L = \{O_L, \boldsymbol{x}_L, \boldsymbol{y}_L, \boldsymbol{z}_L\}$ rigidly attached to it, where O_L is the load center of mass (CoM). Then, we define an inertial frame $\mathcal{F}_W = \{O_W, \boldsymbol{x}_W, \boldsymbol{y}_W, \boldsymbol{z}_W\}$ with $\boldsymbol{z}_W$ oriented in the opposite direction to the gravity vector. The configuration of the load is then described by the position of O_L and orientation of $\mathcal{F}_L$ with respect to $\mathcal{F}_W$, i.e., by the vector $\boldsymbol{p}_L \in \mathbb{R}^3$ and the rotation matrix $\boldsymbol{R}_L \in SO(3)$, respectively. Its dynamics is given by the Newton-Euler equations

$$\begin{aligned} m_L\ddot{\boldsymbol{p}}_L &= -m_L g\boldsymbol{e}_3 + \boldsymbol{f}_e \\ \dot{\boldsymbol{R}}_L &= \boldsymbol{S}(\boldsymbol{\omega}_L)\boldsymbol{R}_L \\ \boldsymbol{J}_L\dot{\boldsymbol{\omega}}_L &= -\boldsymbol{S}(\boldsymbol{\omega}_L)\boldsymbol{J}_L\boldsymbol{\omega}_L + \boldsymbol{\tau}_e - \boldsymbol{\omega}_L^\top\boldsymbol{B}_L\boldsymbol{\omega}_L, \end{aligned}$$

where, $\boldsymbol{\omega}_L \in \mathbb{R}^3$ is the angular velocity of $\mathcal{F}_L$ w.r.t. $\mathcal{F}_W$ expressed in $\mathcal{F}_L$, $\boldsymbol{S}(\star)$ is the operator such that $\boldsymbol{S}(\boldsymbol{x})\boldsymbol{y} = \boldsymbol{x}\times\boldsymbol{y}$, g is the gravitational constant, $\boldsymbol{e}_i$ is the canonical unit vector with a 1 in the i-th entry, $\boldsymbol{f}_e$ and $\boldsymbol{\tau}_e \in \mathbb{R}^3$ are the sum of external forces and moments acting on the load, respectively. The positive definite matrix $\boldsymbol{B}_L \in \mathbb{R}^{3\times3}$ is a damping factor modeling the energy dissipation phenomena.

The load is transported by two aerial robots by means of two cables, one for each robot. We denote with A_i the attachment point of the i-th cable to the i-th robot, with $i = 1, 2$, and we define the frame $\mathcal{F}_{Ri} = \{A_i, \boldsymbol{x}_{Ri}, \boldsymbol{y}_{Ri}, \boldsymbol{z}_{Ri}\}$ rigidly attached to the robot and centered in the attachment point. The i-th robot configuration is described by the position of A_i and orientation of $\mathcal{F}_{Ri}$ w.r.t. $\mathcal{F}_W$, denoted by the vector $\boldsymbol{p}_{Ri} \in \mathbb{R}^3$, and the rotation matrix $\boldsymbol{R}_{Ri} \in SO(3)$, respectively. We assume that a position controller is applied to the aerial robot, able to track any C^2 trajectory with negligible error in the domain of interest, independently from external disturbances. Indeed, with the recent robust controllers (as the one in [15] for both unidirectional- and multidirectional-thrust vehicles) and disturbance observers for aerial vehicles, one can obtain very precise motions, even in the presence of external disturbances. However, the proposed control method results particularly robust to non-ideality, thanks to its passivity nature (see Section V). As a consequence, in real applications, a precise tracking is actually not needed for the stability, but only to achieve perfect performance.

The closed loop translational dynamics of the robot subject to the position controller is then assumed as the one of a double integrator: $\ddot{\boldsymbol{p}}_{Ri} = \boldsymbol{u}_{Ri}$, where $\boldsymbol{u}_{Ri}$ is a virtual input to be designed. If we consider a multidirectional-thrust platform capable of controlling both position and orientation independently [16], the double integrator is an exact model of the closed loop system apart from modeling errors. In the case of underactuated unidirectional-thrust vehicle, the double integrator is instead a very good approximation. Indeed the rotational dynamics is totally decoupled from the translational one and it is much faster than the latter, allowing to apply the time-scale separation principle. At this stage it might seem that the platform is 'infinitely stiff' w.r.t. the force produced by the cable. However, we shall re-introduce a compliant behavior by suitably designing the input $\boldsymbol{u}_{Ri}$.

The other end of the i-th cable is attached to the load at the anchoring point B_i described by the vector ${}^L\boldsymbol{b}_i \in \mathbb{R}^3$ denoting its position with respect to $\mathcal{F}_L$. The position of B_i w.r.t. $\mathcal{F}_W$ is then given by $\boldsymbol{b}_i = \boldsymbol{p}_L + \boldsymbol{R}_L{}^L\boldsymbol{b}_i$. To simplify the discussion we assume, without loss of generality, that ${}^L\boldsymbol{b}_1 = [\|{}^L\boldsymbol{b}_1\|\ 0\ 0]^\top$.

Assumption 1: The two anchoring points are placed such that the load CoM coincides with their middle point, i.e., ${}^L\boldsymbol{b}_1 = -{}^L\boldsymbol{b}_2$. This assumption is rather easy to meet in practice.

We model the i-th cable as a unilateral spring along its principal direction, characterized by a constant elastic coefficient $k_i \in \mathbb{R}_{>0}$, a constant nominal length denoted by l_{0i} and a negligible mass and inertia w.r.t. the ones of the robots and of the load. The attitude of the cable is described by the normalized vector, $\boldsymbol{n}_i = \boldsymbol{l}_i/||\boldsymbol{l}_i||$, where $\boldsymbol{l}_i = \boldsymbol{p}_{Ri} - \boldsymbol{b}_i$. Given a certain elongation $||\boldsymbol{l}_i||$ of the cable, the latter produces a force acting on the load at B_i equal to:

$$\boldsymbol{f}_i = t_i\boldsymbol{n}_i, \quad t_i = \begin{cases} k_i(||\boldsymbol{l}_i|| - l_{0i}) & \text{if } ||\boldsymbol{l}_i|| - l_{0i} > 0 \\ 0 & \text{otherwise} \end{cases}. \tag{1}$$

$t_i \in \mathbb{R}_{\geq0}$ denotes the tension along the cable and it is given by the simplified Hooke's law. As usually done in the related literature, we assume that the controller and the gravity force always maintain the cables taut, at least in the domain of interest. The force produced at the other hand of the cable, namely on the i-th robot at A_i, is equal to $-\boldsymbol{f}_i$.

Considering the forces that robots and load exchange by means of the cables, the dynamics of the full system is:

$$\begin{aligned} \dot{\boldsymbol{v}}_R &= \boldsymbol{u}_R \\ \dot{\boldsymbol{v}}_L &= \boldsymbol{M}_L^{-1}\left(-\boldsymbol{c}_L(\boldsymbol{v}_L) + \boldsymbol{g}_L + \boldsymbol{G}(\boldsymbol{q}_L)\boldsymbol{f}\right), \end{aligned} \tag{2}$$

where $\boldsymbol{q}_R = [\boldsymbol{p}_{R1}^\top\ \boldsymbol{p}_{R2}^\top]^\top$, $\boldsymbol{q}_L = (\boldsymbol{p}_L, \boldsymbol{R}_L)$, $\boldsymbol{v}_R = [\dot{\boldsymbol{p}}_{R1}^\top\ \dot{\boldsymbol{p}}_{R2}^\top]^\top$, $\boldsymbol{v}_L = [\dot{\boldsymbol{p}}_L^\top\ \boldsymbol{\omega}_L^\top]^\top$, $\boldsymbol{u}_R = [\boldsymbol{u}_{R1}^\top\ \boldsymbol{u}_{R2}^\top]^\top$, $\boldsymbol{f} = [\boldsymbol{f}_1^\top\ \boldsymbol{f}_2^\top]^\top$ where $\boldsymbol{f}_i$ is given in (1), and is a function of the state, $\boldsymbol{M}_L = \mathrm{diag}\,(m_L\boldsymbol{I}_3, \boldsymbol{J}_L)$ and $\boldsymbol{I}_3 \in \mathbb{R}^{3\times3}$ the identity matrix, $\boldsymbol{g}_L =$

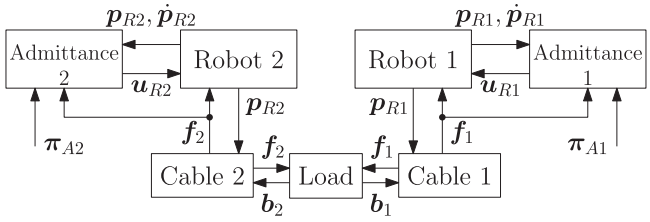

Fig. 2. Schematic representation of the overall system including both physical and control blocks.

$[-m_L g \boldsymbol{e}_3^\top \ \boldsymbol{0}]^\top$, $\boldsymbol{c}_L = [\boldsymbol{0} \ \boldsymbol{S}(\boldsymbol{\omega}_L)\boldsymbol{J}_L\boldsymbol{\omega}_L - \boldsymbol{\omega}_L^\top \boldsymbol{B}_L \boldsymbol{\omega}_L]^\top$ and

$$\boldsymbol{G} = \begin{bmatrix} \boldsymbol{I}_3 & \boldsymbol{I}_3 \\ \boldsymbol{S}({}^L\boldsymbol{b}_1)\boldsymbol{R}_L^\top & \boldsymbol{S}({}^L\boldsymbol{b}_2)\boldsymbol{R}_L^\top \end{bmatrix}.$$

We remark that the two dynamics in (2) are coupled together by the cable forces in (1).

Control Problem

In this work we aim to: i) stabilize the load at a desired configuration, $\bar{\boldsymbol{q}}_L = (\bar{\boldsymbol{p}}_L, \bar{\boldsymbol{R}}_L)$; ii) preserve the stability of the load during its transportation.

Assuming a perfect knowledge of the system dynamic model, and a perfect state estimation, one could use a centralized control approach, as in [8], [9]. We are instead interested in solving the mentioned objectives using a decentralized approach without explicit communication between the robots.

III. Control Design and Equilibria

To achieve the previous control objectives we propose the use of an admittance filter for *both* robots, i.e., setting:

$$\boldsymbol{u}_{Ri} = \boldsymbol{M}_{Ai}^{-1}\left(-\boldsymbol{B}_{Ai}\dot{\boldsymbol{p}}_{Ri} - \boldsymbol{K}_{Ai}\boldsymbol{p}_{Ri} - \boldsymbol{f}_i + \boldsymbol{\pi}_{Ai}\right), \quad (3)$$

where the three positive definite symmetric matrices $\boldsymbol{M}_{Ai}, \boldsymbol{B}_{Ai}, \boldsymbol{K}_{Ai} \in \mathbb{R}^{3\times 3}$ are the virtual inertia of the robot, the virtual damping, and the stiffness of a virtual spring attached to the robot, and $\boldsymbol{\pi}_{Ai} \in \mathbb{R}^3$ is an additional input (see Fig. 2 for a schematic representation). Notice that (3) does not require explicit communication. Indeed it requires only local information, i.e., the state of the robot $(\boldsymbol{p}_{Ri}, \dot{\boldsymbol{p}}_{Ri})$, and the force applied by the cable $\boldsymbol{f}_i$. The first can be retrieved with standard on-board sensors, while the second can be directly measured by an on-board force sensor or estimated by a sufficiently precise model-based observer as done in [13], [16].

Combining equations (2) and (3) we can write the closed loop system dynamics as $\dot{\boldsymbol{v}} = m(\boldsymbol{q}, \boldsymbol{v}, \boldsymbol{\pi}_A)$ where

$$m(\boldsymbol{q}, \boldsymbol{v}, \boldsymbol{\pi}_A) = \begin{bmatrix} \boldsymbol{M}_A^{-1}\left(-\boldsymbol{B}_A\dot{\boldsymbol{p}}_R - \boldsymbol{K}_A\boldsymbol{p}_R - \boldsymbol{f} + \boldsymbol{\pi}_A\right) \\ \boldsymbol{M}_L^{-1}\left(-\boldsymbol{c}_L(\boldsymbol{v}_L) + \boldsymbol{g}_L + \boldsymbol{G}\boldsymbol{f}\right) \end{bmatrix}, \quad (4)$$

with $\boldsymbol{q} = (\boldsymbol{q}_R, \boldsymbol{q}_L)$, $\boldsymbol{v} = [\boldsymbol{v}_R^\top \ \boldsymbol{v}_L^\top]^\top$ and $\boldsymbol{\pi}_A = [\boldsymbol{\pi}_{A1}^\top \ \boldsymbol{\pi}_{A2}^\top]^\top$. Furthermore $\boldsymbol{M}_A = \mathrm{diag}(\boldsymbol{M}_{A1}, \boldsymbol{M}_{A2})$, $\boldsymbol{B}_A = \mathrm{diag}(\boldsymbol{B}_{A1}, \boldsymbol{B}_{A2})$ and $\boldsymbol{K}_A = \mathrm{diag}(\boldsymbol{K}_{A1}, \boldsymbol{K}_{A2})$. In order to coordinate the motions of the robots in a decentralized way we propose a master-slave approach. Only one robot, namely the designated master, will have an active control of the system.

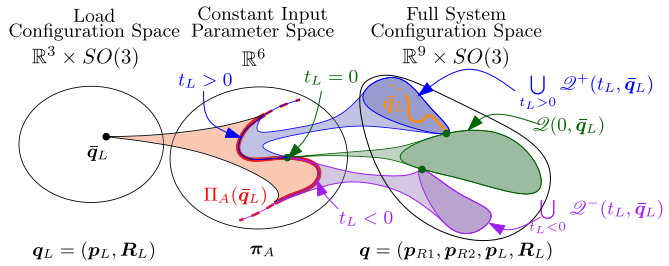

Fig. 3. Relation between the equilibria and forcing control input. In particular, starting from the left: to a desired load configuration of equilibrium it corresponds a forcing input in the subset $\Pi_A(\bar{\boldsymbol{q}}_L)$ of dimension one (inverse problem). Then, moving to the right: to a forcing input in $\Pi_A(\bar{\boldsymbol{q}}_L)$, it corresponds an equilibrium in the subsets $\mathcal{Q}^+(t_L, \bar{\boldsymbol{q}}_L)$, $\mathcal{Q}^-(t_L, \bar{\boldsymbol{q}}_L)$ or $\mathcal{Q}(0, \bar{\boldsymbol{q}}_L)$ according to the value of t_L (direct problem). The orange line inside $\mathcal{Q}^+(t_L, \bar{\boldsymbol{q}}_L)$ corresponds to the equilibria $\boldsymbol{q} \in \mathcal{Q}^+(t_L, \bar{\boldsymbol{q}}_L)$ such that $\boldsymbol{q}_L = \bar{\boldsymbol{q}}_L$.

Choosing robot 1 as master and robot 2 as slave we set $\boldsymbol{K}_{A1} \neq \boldsymbol{0}$, $\boldsymbol{K}_{A2} = \boldsymbol{0}$.

We say that $\boldsymbol{q}$ is an *equilibrium configuration* if $\exists\ \boldsymbol{\pi}_A$ s.t. $\boldsymbol{0} = m(\boldsymbol{q}, \boldsymbol{0}, \boldsymbol{\pi}_A)$, i.e., if the corresponding zero-velocity state $(\boldsymbol{q}, \boldsymbol{0})$ is a forced equilibrium for the system (4) for a certain forcing input $\boldsymbol{\pi}_A$. We say that an equilibrium configuration $\boldsymbol{q}$ is stable, unstable, or asymptotically stable if $(\boldsymbol{q}, \boldsymbol{0})$ is stable, unstable, or asymptotically stable, respectively.

In the following we shall prove that for any desired load configuration $\bar{\boldsymbol{q}}_L$ there exists a set $\Pi_A(\bar{\boldsymbol{q}}_L) \subset \mathbb{R}^6$ such that for any $\boldsymbol{\pi}_A \in \Pi_A(\bar{\boldsymbol{q}}_L)$ one can compute a $\bar{\boldsymbol{q}}_R$, depending on $\bar{\boldsymbol{q}}_L$ and $\boldsymbol{\pi}_A$, that makes $\bar{\boldsymbol{q}} = (\bar{\boldsymbol{q}}_L, \bar{\boldsymbol{q}}_R)$ an asymptotically stable equilibrium with $\boldsymbol{\pi}_A$ as forcing input. As we shall see, a key role in all the following analyses is played by the *load internal force*, defined as

$$t_L := \tfrac{1}{2}\boldsymbol{f}^\top \begin{bmatrix} \boldsymbol{I}_3 & -\boldsymbol{I}_3 \end{bmatrix}^\top \boldsymbol{R}_L \boldsymbol{e}_1 =: \tfrac{1}{2}\boldsymbol{f}^\top \boldsymbol{r}_L, \quad (5)$$

where $\boldsymbol{r}_L = \begin{bmatrix} \boldsymbol{I}_3 & -\boldsymbol{I}_3 \end{bmatrix}^\top \bar{\boldsymbol{R}}_L \boldsymbol{e}_1$. We have that if $t_L > 0$ the internal force is a *tension* (the work of the internal force is positive if the distance between the anchoring points increases) while if $t_L < 0$ the internal force is a *compression* (viceversa, the work is positive if the distance decreases).

A. Equilibrium Configurations of the Closed-Loop System

We firstly carefully analyze the relation between equilibrium configurations, from now on simply called *equilibria*, and the forcing input $\boldsymbol{\pi}_A$. In particular, we shall study: i) *equilibria inverse problem*: which is the *set of inputs* (and corresponding robot positions) that equilibrates a desired $\bar{\boldsymbol{q}}_L$ (Theorem 1); ii) *equilibria direct problem*: which is the *set of equilibria* if $\boldsymbol{\pi}_A$, chosen in the aforementioned set, is applied to the system (Theorem 2). A schematic representation of the results described in the theorems is given in Fig. 3.

Theorem 1 (equilibria inverse problem): Consider the closed loop system (4) and assume that the load is at a given desired configuration $\boldsymbol{q}_L = \bar{\boldsymbol{q}}_L = (\bar{\boldsymbol{p}}_L, \bar{\boldsymbol{R}}_L)$. For each internal force $t_L \in \mathbb{R}$, there exists a unique constant value for the forcing input $\boldsymbol{\pi}_A = \bar{\boldsymbol{\pi}}_A$ (and a unique position of the robots $\boldsymbol{q}_R = \bar{\boldsymbol{q}}_R$) such that $\bar{\boldsymbol{q}} = (\bar{\boldsymbol{q}}_L, \bar{\boldsymbol{q}}_R)$ is an equilibrium of the system.

In particular $\bar{\boldsymbol{\pi}}_A$ and $\bar{\boldsymbol{q}}_R = [\bar{\boldsymbol{p}}_{R1}^\top \ \bar{\boldsymbol{p}}_{R2}^\top]^\top$ are given by

$$\bar{\boldsymbol{\pi}}_A(\bar{\boldsymbol{q}}_L, t_L) = \boldsymbol{K}_A \bar{\boldsymbol{q}}_R + \bar{\boldsymbol{f}}(\bar{\boldsymbol{q}}_L, t_L) \tag{6}$$

$$\bar{\boldsymbol{p}}_{Ri}(\bar{\boldsymbol{q}}_L, t_L) = \bar{\boldsymbol{p}}_L + \bar{\boldsymbol{R}}_L {}^L\boldsymbol{b}_i + \left(\frac{||\bar{\boldsymbol{f}}_i||}{k_i} + l_{0i}\right)\frac{\bar{\boldsymbol{f}}_i}{||\bar{\boldsymbol{f}}_i||}, \tag{7}$$

for $i = 1, 2$, where

$$\bar{\boldsymbol{f}}(\bar{\boldsymbol{q}}_L, t_L) = \begin{bmatrix}\bar{\boldsymbol{f}}_1 \\ \bar{\boldsymbol{f}}_2\end{bmatrix} = \frac{m_L g}{2}\begin{bmatrix}\boldsymbol{I}_3 \\ \boldsymbol{I}_3\end{bmatrix}\boldsymbol{e}_3 + t_L \begin{bmatrix}\boldsymbol{I}_3 \\ -\boldsymbol{I}_3\end{bmatrix}\bar{\boldsymbol{R}}_L \boldsymbol{e}_1. \tag{8}$$

Proof: The desired load configuration $\bar{\boldsymbol{q}}_L$ can be equilibrated if there exists at least a $\bar{\boldsymbol{q}}_R$ and a $\boldsymbol{\pi}_A$ such that:

$$m(\bar{\boldsymbol{q}}, \boldsymbol{0}, \boldsymbol{\pi}_A) = \boldsymbol{0}. \tag{9}$$

Consider the last six rows of (9). We must find the $\boldsymbol{f}$ solving

$$\boldsymbol{G}\boldsymbol{f} = \boldsymbol{g}_L. \tag{10}$$

$\boldsymbol{G}$ is not invertible since $\text{rank}(\boldsymbol{G}) = 5$, thus we have to verify that a solution for (10) exists. Expanding (10) we obtain

$$\boldsymbol{f}_1 + \boldsymbol{f}_2 = +m_{Lge_3} \tag{11}$$

$$\boldsymbol{S}({}^L\boldsymbol{b}_1)\bar{\boldsymbol{R}}_L^\top \boldsymbol{f}_1 + \boldsymbol{S}({}^L\boldsymbol{b}_2)\bar{\boldsymbol{R}}_L^\top \boldsymbol{f}_2 = \boldsymbol{0}. \tag{12}$$

Then, substituting in (12) the $\boldsymbol{f}_1$ obtained from (11) we have $2\boldsymbol{S}({}^L\boldsymbol{b}_1)\bar{\boldsymbol{R}}_L^\top \boldsymbol{f}_2 = +\boldsymbol{S}({}^L\boldsymbol{b}_1)\bar{\boldsymbol{R}}_L^\top m_{Lge3}$, for which $\boldsymbol{f}_2 = m_L g \boldsymbol{e}_3/2$ is always a solution. Therefore, all the solutions of (10) can be written as

$$\bar{\boldsymbol{f}} = \boldsymbol{G}^\dagger \boldsymbol{g}_L + \boldsymbol{r}_L t_L, \tag{13}$$

where $\boldsymbol{G}^\dagger = 1/2[\boldsymbol{I}_3 \ \ \boldsymbol{I}_3]^\top$ is the pseudo inverse of $\boldsymbol{G}$, $\boldsymbol{r}_L \in \mathbb{R}^6$ is a vector in $\text{Null}(\boldsymbol{G})$, and $t_L \in \mathbb{R}$ is an arbitrary number.

We computed $\boldsymbol{r}_L = [\boldsymbol{f}_1^\top \ \ \boldsymbol{f}_2^\top]^\top$ from (11) and (12) imposing the right hand side equal to zero. From (11) $\boldsymbol{f}_2 = -\boldsymbol{f}_1$, and replacing it into (12) we obtain $\boldsymbol{S}(2{}^L\boldsymbol{b}_1)\bar{\boldsymbol{R}}_L^\top \boldsymbol{f}_1 = \boldsymbol{0}$ which is verified if $\boldsymbol{f}_1 = t_L \bar{\boldsymbol{R}}_L \boldsymbol{e}_1$ with $t_L \in \mathbb{R}$. Finally we obtain $\boldsymbol{r}_L = \begin{bmatrix}\boldsymbol{I}_3 & -\boldsymbol{I}_3\end{bmatrix}^\top \bar{\boldsymbol{R}}_L \boldsymbol{e}_1$, as in the definition (5).

Equation (13) can be then rewritten as (8). The expression of $\bar{\boldsymbol{p}}_{Ri}$ in (7) is computed using (1) and the kinematics of the system. Notice that (7) is singular when $\bar{\boldsymbol{f}}_i = \boldsymbol{0}$ for some i. However this can always be avoided properly choosing t_L.

Lastly, from the first six rows of (9) we have that $\bar{\boldsymbol{q}}_L$ is equilibrated if $\boldsymbol{\pi}_A = \bar{\boldsymbol{\pi}}_A$, where $\bar{\boldsymbol{\pi}}_A$ is defined as in (6). □

Remark 1: Based on Theorem 1 we can define a set $\Pi_A(\bar{\boldsymbol{q}}_L) = \{\boldsymbol{\pi}_A \in \mathbb{R}^6 \ : \ \boldsymbol{\pi}_A = \bar{\boldsymbol{\pi}}_A(\bar{\boldsymbol{q}}_L, t_L) \text{ for } t_L \in \mathbb{R}\}$ which has dimension 1, since it is parametrized by the scalar $t_L \in \mathbb{R}$.

Remark 2: Given a desired load configuration $\bar{\boldsymbol{q}}_L$ to equilibrate, Theorem 1 and its constructive proofs give an intuitive method for choosing the forcing input $\boldsymbol{\pi}_A$. In particular one has to choose only the value of the internal force t_L.

Once t_L is chosen and the input $\boldsymbol{\pi}_A = \bar{\boldsymbol{\pi}}_A(t_L, \bar{\boldsymbol{q}}_L)$ is applied to the system, it is not in general granted that $(\bar{\boldsymbol{q}}_L, \bar{\boldsymbol{q}}_R)$ is the only equilibrium of (4), i.e., the equilibria direct problem may have multiple solutions.

Theorem 2 (equilibria direct problem): Given $t_L \in \mathbb{R}$ and the corresponding $\bar{\boldsymbol{\pi}}_A \in \Pi_A(\bar{\boldsymbol{q}}_L)$ computed as in (6), the equilibria of the system (4), when the input $\boldsymbol{\pi}_A = \bar{\boldsymbol{\pi}}_A(t_L, \bar{\boldsymbol{q}}_L)$ is applied, are all and only the ones described by the following conditions

$$\begin{aligned} t_L \boldsymbol{R}_L \boldsymbol{e}_1 \times \bar{\boldsymbol{R}}_L \boldsymbol{e}_1 &= \boldsymbol{0} \\ \boldsymbol{p}_{R1} &= \bar{\boldsymbol{p}}_{R1} \\ \boldsymbol{p}_L = \boldsymbol{p}_{R1} - \boldsymbol{R}_L {}^L\boldsymbol{b}_1 - \left(\frac{||\bar{\boldsymbol{f}}_1||}{k_1} + l_{01}\right)\frac{\bar{\boldsymbol{f}}_1}{||\bar{\boldsymbol{f}}_1||} &= \bar{\boldsymbol{p}}_L + (\bar{\boldsymbol{R}}_L - \boldsymbol{R}_L){}^L\boldsymbol{b}_1 \\ \boldsymbol{p}_{R2} = \boldsymbol{p}_L + \boldsymbol{R}_L {}^L\boldsymbol{b}_2 + \left(\frac{||\bar{\boldsymbol{f}}_2||}{k_2} + l_{02}\right)\frac{\bar{\boldsymbol{f}}_2}{||\bar{\boldsymbol{f}}_2||}. & \end{aligned} \tag{14}$$

$\mathcal{Q}(t_L, \bar{\boldsymbol{q}}_L)$ denotes the set of configurations respecting (14).

Proof: Given $t_L \in \mathbb{R}$, and $\bar{\boldsymbol{\pi}}_A \in \Pi_A(\bar{\boldsymbol{q}}_L)$, a configuration $\boldsymbol{q}$ is an equilibrium if $m(\boldsymbol{q}, \boldsymbol{0}, \bar{\boldsymbol{\pi}}_A) = \boldsymbol{0}$. The first six rows are $\boldsymbol{K}_A \boldsymbol{q}_R + \boldsymbol{f} - \bar{\boldsymbol{\pi}}_A = \boldsymbol{0}$. Then, from (6) we have that

$$\boldsymbol{f} = \boldsymbol{K}_A(\bar{\boldsymbol{q}}_R - \boldsymbol{q}_R) + \bar{\boldsymbol{f}}. \tag{15}$$

Multiplying both sides of (15) by $\boldsymbol{G}$ and using (10) we obtain $\boldsymbol{G}\boldsymbol{K}_A(\bar{\boldsymbol{q}}_R - \boldsymbol{q}_R) + \boldsymbol{G}\bar{\boldsymbol{f}} = \boldsymbol{g}_L$. Then, using $\boldsymbol{K}_{A2} = \boldsymbol{0}$, and the expression of $\bar{\boldsymbol{f}}$ in (8), we get

$$\begin{bmatrix}\boldsymbol{K}_{A1}\boldsymbol{e}_{R1} \\ \boldsymbol{S}({}^L\boldsymbol{b}_1)\boldsymbol{R}_L \boldsymbol{K}_{A1}\boldsymbol{e}_{R1}\end{bmatrix} + \begin{bmatrix} m_L g \boldsymbol{e}_3 \\ 2\boldsymbol{S}({}^L\boldsymbol{b}_2)\boldsymbol{R}_L^\top \bar{\boldsymbol{R}}_L \boldsymbol{e}_1 t_L\end{bmatrix} = \begin{bmatrix} m_L g \boldsymbol{e}_3 \\ \boldsymbol{0}\end{bmatrix}, \tag{16}$$

where $\boldsymbol{e}_{Ri} = (\bar{\boldsymbol{p}}_{Ri} - \boldsymbol{p}_{Ri})$. The top row of (16) implies that $\boldsymbol{e}_{R1} = \boldsymbol{0}$, hence $\boldsymbol{p}_{R1} = \bar{\boldsymbol{p}}_{R1}$. Replacing $\boldsymbol{e}_{R1} = \boldsymbol{0}$ in the bottom part of (16) we obtain

$$\begin{aligned} \boldsymbol{S}({}^L\boldsymbol{b}_2)\boldsymbol{R}_L^\top \bar{\boldsymbol{R}}_L \boldsymbol{e}_1 t_L = \boldsymbol{0} &\Leftrightarrow \ {}^L\boldsymbol{b}_2 \times \boldsymbol{R}_L^\top \bar{\boldsymbol{R}}_L \boldsymbol{e}_1 t_L = \boldsymbol{0} \\ &\Leftrightarrow \ \boldsymbol{R}_L \boldsymbol{e}_1 \times \bar{\boldsymbol{R}}_L \boldsymbol{e}_1 t_L = \boldsymbol{0}. \end{aligned} \tag{17}$$

We can retrieve $\boldsymbol{p}_L$ and $\boldsymbol{p}_{R2}$, using (1) and the kinematics. □

Remark 3: If $t_L = 0$ the conditions in (17) hold for all the possible load attitudes $\boldsymbol{R}_L \in SO(3)$. This means that $\mathcal{Q}(0, \bar{\boldsymbol{q}}_L)$ contains all the $\boldsymbol{R}_L \in SO(3)$ and the $\boldsymbol{q}_R$, $\boldsymbol{p}_L$ computed from $\boldsymbol{R}_L$ using (14). Fig. 4 (b) illustrates some of these equilibria.

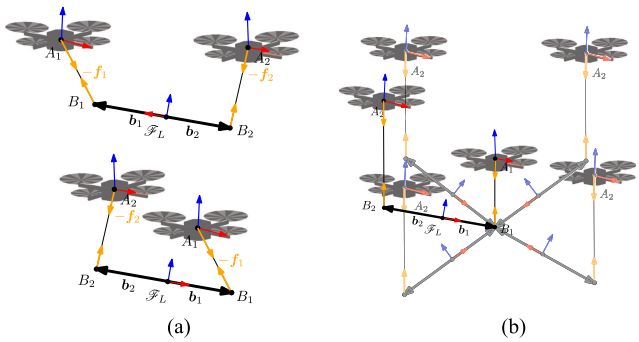

Fig. 4. 2-D representation of the equilibria varying t_L. (a) Two equilibria for $t_L \neq 0$. On the top and on the bottom one equilibrium configuration in $\mathcal{Q}^+(t_L, \bar{\boldsymbol{q}}_L)$ and $\mathcal{Q}^-(t_L, \bar{\boldsymbol{q}}_L)$, respectively. (b) Five of the possible infinite equilibria in $\mathcal{Q}(0, \bar{\boldsymbol{q}}_L)$. In vivid color the configuration $\bar{\boldsymbol{q}}$. The final load pose depends on the initial conditions.

For $t_L \neq 0$, it is required that $\boldsymbol{R}_L \boldsymbol{e}_1$ is parallel to $\bar{\boldsymbol{R}}_L \boldsymbol{e}_1$. This can be obtained with $\boldsymbol{R}_L = \boldsymbol{R}_L(k,\phi) = \bar{\boldsymbol{R}}_L \boldsymbol{R}_{\boldsymbol{z}_L}(k\pi)\boldsymbol{R}_{\boldsymbol{x}_L}(\phi)$, where $k = 0, 1$, $\phi \in [0, 2\pi]$, and $\boldsymbol{R}_{\boldsymbol{z}_L}(\cdot)$ and $\boldsymbol{R}_{\boldsymbol{x}_L}(\cdot)$ are the rotations about $\boldsymbol{z}_L$ and $\boldsymbol{x}_L$, respectively. Considering that ${}^L\boldsymbol{b}_1$ is parallel to $\boldsymbol{x}_L$ we have that $\boldsymbol{R}_{\boldsymbol{z}_L}(k\pi)\boldsymbol{R}_{\boldsymbol{x}_L}(\phi){}^L\boldsymbol{b}_1$ is either equal to ${}^L\boldsymbol{b}_1$ if $k = 0$ or to $-{}^L\boldsymbol{b}_1$ if $k = 1$. Therefore, using (14), we obtain either $\boldsymbol{p}_L = \bar{\boldsymbol{p}}_L$ if $k = 0$ or $\boldsymbol{p}_L = \bar{\boldsymbol{p}}_L + 2\boldsymbol{b}_1$ if $k = 1$. Fig. 4(a) provides a simplified representations of the two different sets of equilibria for $k = 0$ and $k = 1$, formally defined as follows:

- $\mathcal{Q}^+(t_L, \bar{\boldsymbol{q}}_L) = \{\boldsymbol{q} \in \mathcal{Q}(t_L, \bar{\boldsymbol{q}}_L) | \boldsymbol{R}_L = \boldsymbol{R}_L(0,\phi) \forall \phi\}$,
- $\mathcal{Q}^-(t_L, \bar{\boldsymbol{q}}_L) = \{\boldsymbol{q} \in \mathcal{Q}(t_L, \bar{\boldsymbol{q}}_L) | \boldsymbol{R}_L = \boldsymbol{R}_L(1,\phi) \forall \phi\}$.

Notice that $\mathcal{Q}(0, \bar{\boldsymbol{q}}_L)$ is parametrized by an element in $SO(3)$ (any $\boldsymbol{R}_L \in SO(3)$ is allowed), while $\mathcal{Q}^+(t_L, \bar{\boldsymbol{q}}_L)$ and $\mathcal{Q}^-(t_L, \bar{\boldsymbol{q}}_L)$, for $t_L \neq 0$, are parametrized by an element in $SO(1)$ ($\boldsymbol{R}_L(0,\phi)$ and $\boldsymbol{R}_L(1,\phi)$, for any $\phi \in [0, 2\pi]$, respectively). For all t_L, the load rotation about $\boldsymbol{x}_L$ is arbitrary because the robots can not apply any torque along $\boldsymbol{x}_L$, so the corresponding rotation results uncontrollable.

We can conclude that choosing $t_L = 0$ (equilibrium with vertical cables) every orientation of the load is contained in the equilibrium set and the load equilibrium positions are free to move on a sphere of radius $\|{}^L\boldsymbol{b}_1\|$ centered on B_1. Contrarily, $t_L \neq 0$ is a much better choice. In this case, a part from the rotation about the $\boldsymbol{x}_L$ axis, there are only two distinct equilibria, and one is exactly $\boldsymbol{q}_L = \bar{\boldsymbol{q}}_L$, as expected. For the other one the load orientation is parallel to the one in $\bar{\boldsymbol{q}}_L$ but its position is reflected w.r.t. B_1 (see Fig. 4(a) for an example).

IV. Stability of the Equilibria

In this section we shall analyze the stability of the equilibria discovered in Section III-A. Firstly we define $\boldsymbol{x} = (\boldsymbol{q}, \boldsymbol{v})$ as the state of the system, $\bar{\boldsymbol{x}} = (\bar{\boldsymbol{q}}, \boldsymbol{0})$ the desired equilibrium state, and the following sets (subspaces of the state space):

- $\mathscr{X}(t_L, \bar{\boldsymbol{q}}_L) = \{\boldsymbol{x} \ : \ \boldsymbol{q} \in \mathcal{Q}(t_L, \bar{\boldsymbol{q}}_L),\ \boldsymbol{v} = \boldsymbol{0}\}$,
- $\mathscr{X}(0, \bar{\boldsymbol{q}}_L) = \{\boldsymbol{x} \ : \ \boldsymbol{q} \in \mathcal{Q}(0, \bar{\boldsymbol{q}}_L),\ \boldsymbol{v} = \boldsymbol{0}\}$,
- $\mathscr{X}^+(t_L, \bar{\boldsymbol{q}}_L) = \{\boldsymbol{x} \ : \ \boldsymbol{q} \in \mathcal{Q}^+(t_L, \bar{\boldsymbol{q}}_L),\ \boldsymbol{v} = \boldsymbol{0}\}$,
- $\mathscr{X}^-(t_L, \bar{\boldsymbol{q}}_L) = \{\boldsymbol{x} \ : \ \boldsymbol{q} \in \mathcal{Q}^-(t_L, \bar{\boldsymbol{q}}_L),\ \boldsymbol{v} = \boldsymbol{0}\}$.

Theorem 3: Let us consider a desired load configuration $\bar{\boldsymbol{q}}_L$. For the system (4) let the constant forcing input $\boldsymbol{\pi}_A$ be chosen in $\Pi_A(\bar{\boldsymbol{q}}_L)$ corresponding to a certain internal force t_L. Then $\boldsymbol{x}$ belonging to:

- $\mathscr{X}^+(t_L, \bar{\boldsymbol{q}}_L)$ is locally asymptotically stable if $t_L > 0$;
- $\mathscr{X}^-(t_L, \bar{\boldsymbol{q}}_L)$ is unstable if $t_L > 0$;
- $\mathscr{X}(0, \bar{\boldsymbol{q}}_L)$ is locally asymptotically stable;
- $\mathscr{X}^+(t_L, \bar{\boldsymbol{q}}_L)$ is unstable if $t_L < 0$;
- $\mathscr{X}^-(t_L, \bar{\boldsymbol{q}}_L)$ is locally asymptotically stable if $t_L < 0$.

Proof: Let us consider the following Lyapunov candidate:

$$V(\boldsymbol{x}) = \frac{1}{2}(\boldsymbol{v}_R^\top \boldsymbol{M}_A \boldsymbol{v}_R + \boldsymbol{e}_R^\top \boldsymbol{K}_A \boldsymbol{e}_R + \boldsymbol{v}_L^\top \boldsymbol{M}_L \boldsymbol{v}_L + k_1(||\boldsymbol{l}_1|| - l_{01})^2 + k_2(||\boldsymbol{l}_2|| - l_{02})^2) - \boldsymbol{l}_1^\top \bar{\boldsymbol{f}}_1 + - \boldsymbol{l}_2^\top \bar{\boldsymbol{f}}_2 + t_L(1 - (\bar{\boldsymbol{R}}_L \boldsymbol{e}_1)^\top \boldsymbol{R}_L \boldsymbol{e}_1) + V_0, \qquad (18)$$

where $V_0 \in \mathbb{R}_{\geq 0}$ and $\boldsymbol{e}_R = \bar{\boldsymbol{p}}_{R1} - \boldsymbol{p}_{R1}$. For an opportune choice of V_0, $V(\boldsymbol{x})$ is a positive definite, continuously differentiable function in the domain of interest for which we have that $\boldsymbol{x}_{\min} = \operatorname{argmin}_{\boldsymbol{x}} V(\boldsymbol{x})$ is such that $\boldsymbol{x}_{\min} \in \mathscr{X}(0, \bar{\boldsymbol{q}}_L)$ and $\boldsymbol{x}_{\min} \in \mathscr{X}^+(t_L, \bar{\boldsymbol{q}}_L)$ for $t_L > 0$. The complete proof is provided in a technical report in the multimedia materials. In particular, if $t_L \geq 0$, we can choose the term V_0 such that $V(\boldsymbol{x}) \geq 0$ and $V(\bar{\boldsymbol{x}}) = 0$. Notice that $V(\boldsymbol{x}) = 0$ for all $\boldsymbol{x} \in \mathscr{X}(0, \bar{\boldsymbol{q}}_L)$ and $\boldsymbol{x} \in \mathscr{X}^+(t_L, \bar{\boldsymbol{q}}_L)$ for $t_L > 0$.

Computing the time derivative of (18) and replacing (4), (1) and (8) we obtain $\dot{V} = -\boldsymbol{v}_R{}^\top \boldsymbol{B}_A \boldsymbol{v}_R - \boldsymbol{\omega}_L^\top \boldsymbol{B}_L \boldsymbol{\omega}_L$ that is clearly negative semidefinite. In particular $\dot{V}(\boldsymbol{x}) = 0$ for all $\boldsymbol{x} \in \mathcal{E}\{\boldsymbol{x} \ : \ \boldsymbol{v}_R = \boldsymbol{0},\ \boldsymbol{\omega}_L = \boldsymbol{0}\}$

Since $\dot{V}$ is only negative semidefinite, to prove the asymptotic stability we rely on the *LaSalle's invariance principle* [17]. Let us define a positively invariant set $\Omega_\alpha = \{\boldsymbol{x} : V(\boldsymbol{x}) \leq \alpha \text{ with } \alpha \in \mathbb{R}_{>0}\}$. By construction Ω_α is compact since (18) is radially unbounded and Ω_0 is compact ($\Omega_0 = \mathscr{X}(0, \bar{\boldsymbol{q}}_L)$ and $\Omega_0 = \mathscr{X}^+(t_L, \bar{\boldsymbol{q}}_L)$ for $t_L = 0$ and $t_L > 0$, respectively, are both compact sets). Then we need to find the largest invariant set $\mathcal{M}$ in $\mathcal{E} = \{\boldsymbol{x} \in \Omega_\alpha \mid \dot{V}(\boldsymbol{x}) = 0\}$. A trajectory $\boldsymbol{x}(t)$ belongs identically to $\mathcal{E}$ if $\dot{V}(\boldsymbol{x}(t)) \equiv 0 \Leftrightarrow \boldsymbol{v}_R(t) \equiv \boldsymbol{0}$ and $\boldsymbol{\omega}_L(t) \equiv \boldsymbol{0} \Leftrightarrow m(\boldsymbol{q}(t), \boldsymbol{0}, \boldsymbol{\pi}_A) = \boldsymbol{0}$ for all $t \in \mathbb{R}_{>0}$. Therefore $\boldsymbol{x}$ has to be an equilibrium, and from Theorem 2 we have that $\dot{V}(\boldsymbol{x}(t)) \equiv 0 \Leftrightarrow \boldsymbol{x}(t) \in \mathscr{X}(t_L, \bar{\boldsymbol{q}}_L)$. Thus we obtain $\mathcal{M} = \Omega_\alpha \cap \mathscr{X}(t_L, \bar{\boldsymbol{q}}_L)$.

For $t_L > 0$, it is easy to see that for a sufficiently small α, $\mathscr{X}^+(t_L, \bar{\boldsymbol{q}}_L) \subseteq \Omega_\alpha$ but $\mathscr{X}^-(t_L, \bar{\boldsymbol{q}}_L) \cap \Omega_\alpha = \varnothing$. This because $V(\boldsymbol{x}) = 0$ for $\boldsymbol{x} \in \mathscr{X}^+(t_L, \bar{\boldsymbol{q}}_L)$, while $V(\boldsymbol{x}) > 0$ for $\boldsymbol{x} \in \mathscr{X}^-(t_L, \bar{\boldsymbol{q}}_L)$. Indeed, in (18), for $\boldsymbol{x} \in \mathscr{X}^-(t_L, \bar{\boldsymbol{q}}_L)$, the term $t_L(1 - (\bar{\boldsymbol{R}}_L \boldsymbol{e}_1)^\top \boldsymbol{R}_L \boldsymbol{e}_1) = 2t_L > 0$. Therefore $\mathcal{M} = \mathscr{X}^+(t_L, \bar{\boldsymbol{q}}_L)$. All conditions of LaSalle's principle are satisfied and $\mathscr{X}^+(t_L, \bar{\boldsymbol{q}}_L)$ is locally asymptotically stable.

On the other hand, for $t_L = 0$ we have that $\mathscr{X}(t_L, \bar{\boldsymbol{q}}_L) \subseteq \Omega_\alpha$ for every sufficiently small α. Therefore $\mathcal{M} = \mathscr{X}(t_L, \bar{\boldsymbol{q}}_L)$ and, as before, we can conclude that $\mathscr{X}(t_L, \bar{\boldsymbol{q}}_L)$ is locally asymptotically stable for the LaSalle's invariance principle.

Now, let us investigate the stability for $t_L < 0$. As before, with an opportune choice of V_0, we have that $V(\boldsymbol{x}) = 0$ for $\boldsymbol{x} \in \mathscr{X}^+(t_L, \bar{\boldsymbol{q}}_L)$. However, $\mathscr{X}^+(t_L, \bar{\boldsymbol{q}}_L)$ is a set of accumulation for the points where $V(\boldsymbol{x}) < 0$. Indeed, consider $\boldsymbol{v} = \boldsymbol{0}$, $\boldsymbol{p}_{R1} = \bar{\boldsymbol{p}}_{R1}$, $\boldsymbol{R}_L$ such that $(\bar{\boldsymbol{R}}_L \boldsymbol{e}_1)^\top \boldsymbol{R}_L \boldsymbol{e}_1 = 1 - \varepsilon$, with $\varepsilon > 0$ arbitrarily small, $\boldsymbol{p}_L$ and $\boldsymbol{p}_{R2}$ as in (14). Under this conditions, we have that $V(\boldsymbol{x}) = t_L(1 - (\bar{\boldsymbol{R}}_L \boldsymbol{e}_1)^\top \boldsymbol{R}_L \boldsymbol{e}_1) = t_L \varepsilon < 0$. Then, $\dot{V}(\boldsymbol{x}) < 0$ in a neighborhood of $\mathscr{X}^+(t_L, \bar{\boldsymbol{q}}_L)$. All conditions of *Chetaev's theorem* [17] are satisfied, and we can conclude that $\mathscr{X}^+(t_L, \bar{\boldsymbol{q}}_L)$ is an unstable set.

Finally, to study the stability of $\mathscr{X}^-(t_L, \bar{\boldsymbol{q}}_L)$ for $t_L \neq 0$, let us consider a desired load configuration $\bar{\boldsymbol{q}}'_L = (\bar{\boldsymbol{p}}'_L, \bar{\boldsymbol{R}}'_L)$ such that $\bar{\boldsymbol{p}}'_L = \boldsymbol{p}'_L + 2\bar{\boldsymbol{R}}_L \boldsymbol{e}_1$ and $\bar{\boldsymbol{R}}'_L = \boldsymbol{R}_L(1,\phi)$ for a certain ϕ. Then we choose $\boldsymbol{\pi}'_A \in \Pi_A(\bar{\boldsymbol{q}}'_L)$ with $t'_L = -t_L$. For the reasoning in Section III-A, we have that $\mathscr{X}^+(t'_L, \bar{\boldsymbol{q}}'_L) = \mathscr{X}^-(t_L, \bar{\boldsymbol{q}}_L)$. Furthermore, for the previous results, if $t_L > 0$, $t'_L < 0$ and $\mathscr{X}^+(t'_L, \bar{\boldsymbol{q}}'_L)$ is unstable. Therefore, $\mathscr{X}^-(t_L, \bar{\boldsymbol{q}}_L)$ is unstable too. A similar reasoning can be followed to prove that $\mathscr{X}^-(t_L, \bar{\boldsymbol{q}}_L)$ is locally asymptotically stable for $t_L < 0$. □

V. Passivity and Stability of Manipulation

Theorem 3 characterizes the stability of all the possible static equilibria given a certain constant forcing input. In particular, it

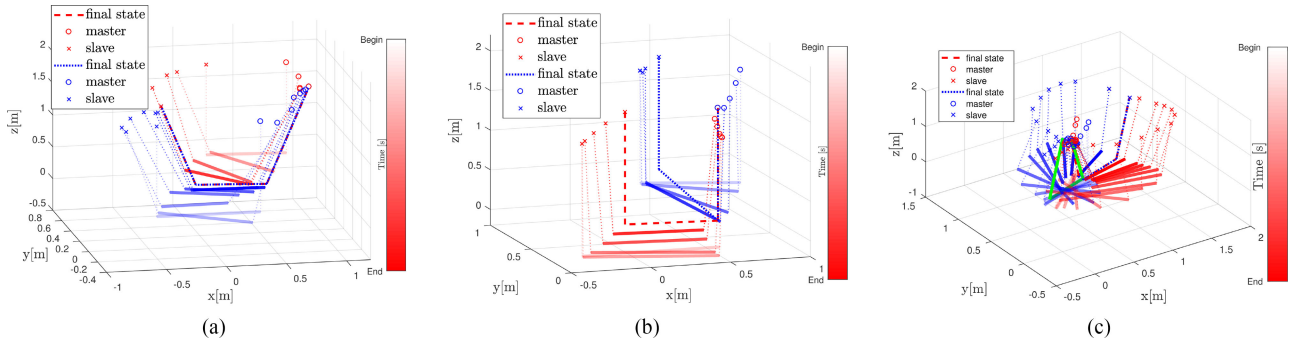

(a) (b) (c)

Fig. 5. Each figure shows the evolution of the system from two different initial conditions (one is shown in red and the other in blue). The two evolutions are represented as a sequence of images discriminated by the brightness of the color that represents the time (from bright/start to dark/end). The load is represented as a tick solid line, the cables as thin dashed lines, the master robot as a circle and the slave robot as a cross. (a) $t_L = t_{L1} > 0$. (b) $t_L = t_{L2} = 0$. (c) $t_L = t_{L3} < 0$.

shows that one has to choose $t_L > 0$ and $\boldsymbol{\pi}_A \in \Pi_A(\bar{\boldsymbol{q}}_L)$ to let the system asymptotically converge to a desired load configuration. On the contrary, one must avoid $t_L = 0$ because the control of the load attitude and its position is not possible. Notice that this last case is the most used in the literature, where the attempt is made to keep the cables always vertical, i.e., with no internal forces.

Let us now show how one can exploit the input $\boldsymbol{\pi}_{A1}$ in order to move the load between two distinct positions. From (6)–(8) and from the fact that $\boldsymbol{K}_{A2} = \boldsymbol{0}$, it descends that only $\bar{\boldsymbol{\pi}}_{A1}$, in $\bar{\boldsymbol{\pi}}_A = [\bar{\boldsymbol{\pi}}_{A1}^\top \ \bar{\boldsymbol{\pi}}_{A2}^\top]^\top$, actually depends on the desired load position $\bar{\boldsymbol{p}}_L$. This makes robot 1 able to steer alone the load position without communicating with robot 2. This is done by first plugging a new desired position $\bar{\boldsymbol{p}}'_L$ in (6) thus computing a new $\bar{\boldsymbol{p}}'_{R1}$, and then plugging $\bar{\boldsymbol{p}}'_{R1}$ in (7) in order to compute the new constant forcing input $\bar{\boldsymbol{\pi}}'_{A1}$. However, one may want to minimize the transient phases generated by a piecewise constant forcing input. It is sufficient to design $\boldsymbol{\pi}_{A1}$ as

$$\boldsymbol{\pi}_{A1}(t) = \bar{\boldsymbol{\pi}}_{A1} + \boldsymbol{u}_{A1}(t), \tag{19}$$

where $\boldsymbol{u}_{A1}(t)$ is a smooth function such that $\boldsymbol{\pi}_{A1}(0) = \bar{\boldsymbol{\pi}}_{A1}$ and $\boldsymbol{\pi}_{A1}(t_f) = \bar{\boldsymbol{\pi}}'_{A1}$ for $t_f \in \mathbb{R}_{>0}$.

To ensure that the system remains stable when the input is time-varying, we shall prove that the system is output-strictly passive w.r.t. the input-output pair $(\boldsymbol{u}, \boldsymbol{y}) = (\boldsymbol{u}_A, \boldsymbol{v}_R)$.

Theorem 4: If $\boldsymbol{\pi}_A$ is defined as in (19) for a certain $\bar{\boldsymbol{q}}$ and $\bar{\boldsymbol{q}}'$ with $t_L \geq 0$, then system (4) is output-strictly passive w.r.t. the storage function (18) and the input-output pair $(\boldsymbol{u}, \boldsymbol{y}) = (\boldsymbol{u}_A, \ \boldsymbol{v}_R)$.

Proof: In the proof of Theorem 3 we already shown that (18) is a continuously differentiable positive definite function for $t_L \geq 0$, properly choosing V_0. Furthermore, replacing (19) into (3), and differentiating (18) we obtain

$$\begin{aligned} \dot{V} = & -\boldsymbol{v}_R{}^\top \boldsymbol{B}_A \boldsymbol{v}_R + \boldsymbol{v}_R{}^\top \boldsymbol{u}_A - \boldsymbol{\omega}_L^\top \boldsymbol{B}_L \boldsymbol{\omega}_L \\ & \leq \boldsymbol{u}^\top \boldsymbol{y} - \boldsymbol{y}^\top \boldsymbol{B}_A \boldsymbol{y} = \boldsymbol{u}^\top \boldsymbol{y} - \boldsymbol{y}^\top \boldsymbol{\Phi}(\boldsymbol{y}), \end{aligned} \tag{20}$$

with $\boldsymbol{y}^\top \boldsymbol{\Phi}(\boldsymbol{y}) > 0 \ \forall \ \boldsymbol{y} \neq \boldsymbol{0}$. Therefore, system (4) is *output-strictly passive* [17]. □

Thanks to the passivity of the system we can say that for a bounded input provided to the master, the energy of the system remains bounded too, and in particular it stabilizes to a new constant value as soon as $\boldsymbol{u}_{A1}$ becomes constant again.

TABLE I
PARAMETERS USED IN THE SIMULATIONS

System Parameters			Controller Gains		
	$i=1$	$i=2$		$i=1$	$i=2$
m_{Ri} [Kg]	1.02	0.993	$\boldsymbol{M}_{Ai}$	$3\boldsymbol{I}_3$	$0.5\boldsymbol{I}_3$
$\boldsymbol{J}_{Ri}$ [Kg·m^2]	$0.015\boldsymbol{I}_3$	$0.015\boldsymbol{I}_3$	$\boldsymbol{B}_{Ai}$	$18\boldsymbol{I}_3$	$1.3\boldsymbol{I}_3$
l_{0i} [m]	1	1	$\boldsymbol{K}_{Ai}$	$15\boldsymbol{I}_3$	$\boldsymbol{0}$
k_i [N/m]	20	20	Desired Load Pose		
${}^L\boldsymbol{b}_i$ [m]	[0.433 0 0]	[−0.433 0 0]	$\bar{\boldsymbol{p}}_L = [0.3 \ 0.3 \ 0.2]^\top$ [m]		
$m_L = 0.900$ [Kg], $\boldsymbol{J}_{Lx} = 0.112$ [Kg·m^2]			$\bar{\phi} = 0$, $\bar{\theta} = \pi/8$ [rad]		
$\boldsymbol{J}_{Ly} = 5.681$, $\boldsymbol{J}_{Lz} = 5.681$ [Kg·m^2]			$\bar{\psi} = \pi/7$ [rad]		

This means that, while moving the master, the overall state of the system will remain bounded, and will converge to another specific equilibrium configuration when the master input becomes constant. Furthermore, it is well known that passivity is a robust property, especially w.r.t. model uncertainties. In particular, choosing $\boldsymbol{\pi}_A \in \Pi_A(\bar{\boldsymbol{q}}_L)$ for a given $\bar{\boldsymbol{q}}$, the system remains asymptotically stable even in the presence of some parameter uncertainties, but it will converge to a $\bar{\boldsymbol{q}}'$ that is slightly different from $\bar{\boldsymbol{q}}$.

Remark 4: Once the desired load pose is decided and the value of t_L is chosen, one can compute the control input $\boldsymbol{\pi}_A$ and send it to the robots. Afterwards, if $t_L > 0$ the robots will steer the load to the desired configuration preserving the stability and without the need of sending data to each other. The cooperative task is performed exploiting the implicit communication through the forces that the robots exchange and feel from the cables and the object.

VI. NUMERICAL VALIDATION

In this section we shall describe the results of several numerical simulations validating the proposed method and all the presented theoretical concepts and results.

For the simulation we considered a quadrotor-like vehicle with its proper nonlinear dynamics together with a geometric position controller, even though, our method can be applied to more general flying vehicles. System and control parameters are reported in Table I. Notice the smaller apparent inertia of the slave, chosen to make it more sensitive to external forces.

Let us consider the desired equilibrium $\bar{\boldsymbol{q}} = (\bar{\boldsymbol{p}}_L, \bar{\boldsymbol{R}}_L)$, whose value are in Table I, where $(\bar{\phi}, \bar{\theta}, \bar{\psi})$ are the Euler angles that

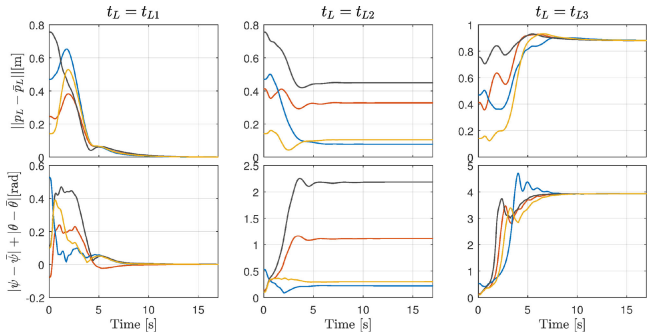

Fig. 6. Convergence to the desired load configuration for cases 1–3. In particular, the first and second rows show the position and the attitude errors, respectively, for four different initial conditions (different colors) and for the three different internal force values (columns). The attitude error is computed as the sum of pitch and yaw errors. The roll error is not considered since it is not controllable.

parametrize $\bar{\boldsymbol{R}}_L$. We performed several simulations with $\boldsymbol{\pi}_A \in \Pi_A(\bar{\boldsymbol{q}}_L)$ computed as in (6) for the cases: 1) $t_{L1} = 1.5$ [N] > 0, 2) $t_{L2} = 0$ [N], 3) $t_{L3} = -1$ [N] < 0.

To test the stability of the equilibria, we initialized the system in different initial configurations and we let it evolve. Fig. 6 shows the position and orientation error for the three t_L and several different initial conditions. 1) For $t_L = t_{L1}$, the system always converges to a state belonging to $\mathscr{X}^+(t_L, \bar{\boldsymbol{q}}_L)$, independently from the initial state, validating the asymptotic stability of $\mathscr{X}^+(t_L, \bar{\boldsymbol{q}}_L)$ when $t_L > 0$. 2) For t_{L2}, the system final state belongs to $\mathscr{X}(0, \bar{\boldsymbol{q}}_L)$. The particular final attitude of the load depends on the initial state. 3) For t_{L3}, the system never converges to $\mathscr{X}^+(t_L, \bar{\boldsymbol{q}}_L)$ even with a very close initial configuration. This is due to the instability of $\mathscr{X}^+(t_L, \bar{\boldsymbol{q}}_L)$ when $t_L < 0$. Fig. 5 shows the evolution of the system starting from two different initial states for the three cases.

In another set of simulations, shown in detail in the attached technical report, the master input $\boldsymbol{\pi}_{A1}(t)$ is chosen as in (19) to bring the load in $\bar{\boldsymbol{p}}'_L = [4.5\ 4.5\ 5]^\top$[m]. We observed that, as expected, for both $t_L = t_{L1}$ and $t_L = t_{L2}$ the system remains stable during the master maneuver. Once the input becomes constant, the master stops and the system converges to $\bar{\boldsymbol{q}}$ for $t_L = t_{L1}$. For $t_L = t_{L2}$, the final load attitude depends on the particular motion, and it is in general different from $\bar{\boldsymbol{q}}$.

Additional simulations in non-ideal conditions are provided in the attached technical report. The results show that thanks to the passivity of the system, the latter is very robust to the considered non-idealities. Some representative simulations are available in the attached video too.

VII. Conclusion

This work deals with the decentralized cooperative manipulation of a cable-suspended load performed by two aerial vehicles. The proposed master-slave architecture exploits an admittance controller in order to coordinate the robots with implicit communication only, using the cable forces. The passivity of the system has been proven, and the stability of the static equilibria has been studied highlighting the crucial role of the internal force. In particular, contrarily from what it is normally done in the literature (zero internal force), it is advisable to choose a positive internal force to control both position and orientation of the beam. In the future it would be interesting to test the method on real platforms and to extend the analysis to general loads or to agile motions. An extension to a more generic load attached to N robots could be very interesting too.

References

[1] M. Tognon, B. Yüksel, G. Buondonno, and A. Franchi, "Dynamic decentralized control for protocentric aerial manipulators," in *Proc. IEEE Int. Conf. Robot. Autom.*, Singapore, May 2017, pp. 6375–6380.

[2] M. Tognon, A. Testa, E. Rossi, and A. Franchi, "Takeoff and landing on slopes via inclined hovering with a tethered aerial robot," in *Proc. IEEE/RSJ Int. Conf. Intell. Robots Syst.*, Daejeon, South Korea, Oct. 2016, pp. 1702–1707.

[3] M. Tognon and A. Franchi, "Dynamics, control, and estimation for aerial robots tethered by cables or bars," *IEEE Trans. Robot.*, vol. 33, no. 4, pp. 834–845, Aug. 2017.

[4] I. Maza, K. Kondak, M. Bernard, and A. Ollero, "Multi-UAV cooperation and control for load transportation and deployment," *J. Intell. Robot. Syst.*, vol. 57, nos. 1–4, pp. 417–449, 2010.

[5] H.-N. Nguyen, S. Park, and D. J. Lee, "Aerial tool operation system using quadrotors as rotating thrust generators," in *Proc. IEEE/RSJ Int. Conf. Intell. Robots Syst.*, Hamburg, Germany, Oct. 2015, pp. 1285–1291.

[6] R. Ritz and R. D'Andrea, "Carrying a flexible payload with multiple flying vehicles," in *Proc. IEEE/RSJ Int. Conf. Intell. Robots Syst.*, 2013, pp. 3465–3471.

[7] F. Caccavale, G. Giglio, G. Muscio, and F. Pierri, "Cooperative impedance control for multiple UAVs with a robotic arm," in *Proc. IEEE/RSJ Int. Conf. Intell. Robots Syst.*, 2015, pp. 2366–2371.

[8] K. Sreenath and V. Kumar, "Dynamics, control and planning for cooperative manipulation of payloads suspended by cables from multiple quadrotor robots," in *Proc. Robot.: Sci. Syst. Conf.*, Berlin, Germany, Jun. 2013.

[9] C. Masone, H. H. Bülthoff, and P. Stegagno, "Cooperative transportation of a payload using quadrotors: A reconfigurable cable-driven parallel robot," in *Proc. IEEE/RSJ Int. Conf. Intell. Robots Syst.*, Oct. 2016, pp. 1623–1630.

[10] M. Manubens, D. Devaurs, L. Ros, and J. Cortés, "Motion planning for 6-D manipulation with aerial towed-cable systems," in *Proc. Robot.: Sci. Syst. Conf.*, Berlin, Germany, May 2013.

[11] D. Mellinger, M. Shomin, N. Michael, and V. Kumar, "Cooperative grasping and transport using multiple quadrotors," in *Proc. Int. Symp. Distrib. Auton. Robotic Syst.*, 2013, pp. 545–558.

[12] Z. Wang and M. Schwager, "Force-amplifying n-robot transport system (force-ants) for cooperative planar manipulation without communication," *Int. J. Robot. Res.*, vol. 35, no. 13, pp. 1564–1586, 2016.

[13] A. Tagliabue, M. Kamel, S. Verling, R. Siegwart, and J. Nieto, "Collaborative transportation using MAVs via passive force control," in *Proc. IEEE Int. Conf. Robot. Autom.*, Singapore, 2016, pp. 5766–5773.

[14] M. Gassner, T. Cieslewski, and D. Scaramuzza, "Dynamic collaboration without communication: Vision-based cable-suspended load transport with two quadrotors," in *Proc. IEEE Int. Conf. Robot. Autom.*, Singapore, 2017, pp. 5196–5202.

[15] M. Ryll, D. Bicego, and A. Franchi, "Modeling and control of FAST-Hex: A fully-actuated by synchronized-tilting hexarotor," in *Proc. IEEE/RSJ Int. Conf. Intell. Robots Syst.*, Daejeon, South Korea, Oct. 2016, pp. 1689–1694.

[16] M. Ryll *et al.*, "6D physical interaction with a fully actuated aerial robot," in *Proc. IEEE Int. Conf. Robot. Autom.*, Singapore, May 2017, pp. 5190–5195.

[17] H. K. Khalil, *Nonlinear Systems*, 3rd ed. Englewood Cliffs, NJ, USA: Prentice-Hall, 2001.